Earth Planets Space, **65**, 1563–1568, 2013

Differentiation of silicates from H_2O ice in an icy body induced by ripening

Sin-iti Sirono

Earth and Environmental Sciences, Graduate School of Environmental Sciences, Nagoya University, Nagoya 464-8601, Japan

(Received September 23, 2012; Revised July 1, 2013; Accepted July 8, 2013; Online published December 6, 2013)

One of the probable scenarios of differentiation between silicate-ice in an icy object is the settling of a silicate particle in water after the melting of the object. In order for settling to proceed or occur, the size of the particle should be sufficiently large such that the settling velocity of the particle exceeds the background flow velocity induced by thermal convection. The sizes of the particles change because of dissolution and precipitation. This process is called ripening. In this study, the critical particle sizes required for settling, and the timescales for the growth of the particles to these sizes through ripening, are analytically derived. It is observed that settling is possible if the silicate particles coagulate with each other to form a network in water. If the particles do not coagulate, the probability of the occurrence of settling is low, because the time duration required for the particle growth to the critical size is large. The coagulation of silicate particles strongly depends on the pH of the water.
Key words: Asteroids, ice, ripening.

1. Introduction

The outer regions of the solar system are populated by objects such as icy planets, satellites, and cometary nuclei, along with Kuiper belt objects. The internal structures of several such icy satellites have been estimated by space missions. The process of differentiation is crucial to the internal structure of such objects. Ganymede can be differentiated as an iron core, rock mantle, and icy mantle (Showman and Malhotra, 1999). On the other hand, only a partial differentiation between ice and rock can be made for Callisto (Kuskov and Kronrod, 2005). The most probable scenario for ice–rock differentiation is the gravitational settling of silicate particles after the melting of the silicate-ice mixture in the object. For example, Barr and Canup (2010) investigated the differentiation of Ganymede due to impact melting. They showed the size of a silicate particle settling downward to be larger than 30 μm.

However, it should be noted that the building blocks of the above-mentioned icy objects are interstellar grains which are sub-micron sized icy grains containing silicate cores (Li and Greenberg, 1997). Let us suppose that a sub-micron-sized silicate particle is placed in water. The question is whether the particle can settle down or not. The Stokes settling velocity for water is quite small; it is on the order of 10^{-7} cm s^{-1} inside a 1000-km-radius object. This velocity is obtained from the Stokes's drag law (Eq. (2) shown later with parameters below Eq. (5)). Moreover, this small settling velocity cannot be achieved due to thermal convection inside the object. Therefore, differentiation between silicates and ice is improbable for sub-micron particle sizes.

The size of a silicate particle in water changes through Ostwald ripening (Ratke and Voorhees, 2002). Because the solubility of a small particle is larger than that of a large particle, silicates dissolve into water from small particles and precipitate onto large particles (see Fig. 1(a)). The size distribution gradually changes, and the mean size of the silicates increases. The change in size distribution of clay particles has been observed (Eberl *et al*., 1990). If a particle grows so that the settling proceeds against convection flow, the differentiation process begins.

In this paper, the critical size of a particle for settling is determined, taking into account the coarsening due to Ostwald ripening. Correspondingly, this study has two aspects. One is the determination of the background flow velocity against which a particle settles down. This is achieved using the formulas of convective velocity and of the permeable flow velocity. The other aspect is devoted to calculating the timescale for the particle growth through ripening. Ostwald ripening has been mainly studied in the field of metallurgy. The theoretical framework of Ostwald ripening has been well developed (Ratke and Voorhees, 2002). Moreover, an analytical solution for the evolution of the size distribution, appropriate to the conditions in this study, has been obtained (Kumaran, 1998).

In the next section, the scenario of this model is described, because this study involves several mechanisms which are unfamiliar in the field of geophysics. In Section 3, the critical size for differentiation is analytically derived. In Section 4, the timescale for particle growth is estimated, and the requirement for the composition of ice is discussed in Section 5. Section 6 presents the conclusions.

2. Scenario of This Model

The scenario of this study is schematically displayed in Fig. 1. Here, we assume that a molten layer of an icy object is formed by a heating event. There are several possi-

doi:10.5047/eps.2013.07.002

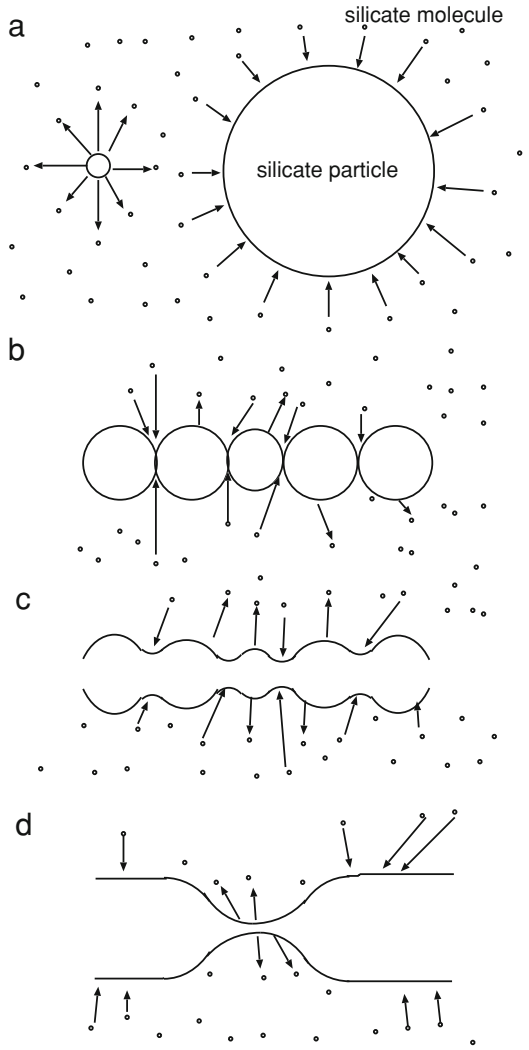

Fig. 1. Schematics of the scenario of this model. (a) Size evolution of silicate particles. Silicate molecules (small circles) dissolve into water from the small silicate particle and precipitate onto the large particle. (b) Evolution of a series of grains. Silicate molecules precipitate onto the necks between grains because of its concave surface. (c) After the necks are filled with silicate molecules, the thickness reflects the initial size of the grains. (d) Splitting occurs at the thin section because of the variation in the surface curvature.

ble origins of the heating event causing the melting. The decay of a radionuclide, such as ^{40}K or ^{26}Al, is a promising mechanism which leads to melting (Prialnik and Merk, 2008). Tidal heating is also a powerful source of heating as seen in Europa's underground ocean (Ross and Schubert, 1987). Impact melting is another reasonable mechanism (Barr and Canup, 2010) because impact is a common event in the planetary formation process. Here, I do not address the origin of the heat source and simply assume the existence of a molten layer of thickness D inside an icy object.

If melting occurs, silicate particles are immersed in water. The constituent molecules dissolve in the water according to their solubility. It should be noted that the solubility depends on the surface curvature (or size) of a given particle. The solubility of a small particle is larger than that of a large particle because of the Gibbs-Thomson effect (Ratke and Voorhees, 2002). As a result, a molecule originates from a small particle and precipitates on a large particle (Fig. 1(a)), leading to a coarsening of the particles. If the settling velocity of the large particle becomes larger than the background flow velocity of water, the settling and differentiation of silicate proceeds.

The discussion above implicitly assumes that each particle is kept isolated without coagulating with other particles. This is true if there is a repulsive interaction between the silicate particles in water. In many cases, the surface of a sub-micron sized particle is charged. The origin of charging is the ionization of the surface material, or ions contained in the water. The former depends on the pH of water, and the latter depends on the amount of salt in the water. Repulsion of particles is caused by the osmotic pressure induced between two approaching particles. This mechanism is summarized as DVLO theory (Safran, 1994). In addition to this mechanism, it is possible that organic molecules formed in the interstellar space are dissolved in the water. This molecule, when absorbed by a particle, may induce steric stabilization of silica particles (Iler, 1979).

On the other hand, there is a particular pH value where the surface charge on the particle is zero. This pH is known as the point of zero charge (PZC). The coagulation of particles efficiently proceeds around PZC. If the amount of salt in the water is large, the osmotic pressure is not induced because the contrast of ion concentration in the gap between the particles disappears and coagulation proceeds.

All of these mechanisms depend on the composition of the water. The composition is determined through the chemical evolution in the molecular cloud and in the protoplanetary nebula, and is highly uncertain. Therefore, only two extreme cases are considered in this paper. One is the case without coagulation of particles. In this case, the particles do not coagulate and remain isolated throughout the evolution. In the other case, coagulation proceeds efficiently. The particles coagulate with each other to form a spanning network throughout the molten layer inside the icy object.

3. Critical Sizes for Settling

3.1 Without coagulation

The formation of a molten layer inside an icy object has been discussed in many studies (Multhaup and Spohn, 2007; Schubert *et al*., 2007; Castillo-Rogez *et al*., 2012; Czechowski, 2012). Heating by the decay of ^{26}Al efficiently melts the interior of Rhea, a Saturnian satellite with a radius of 764 km (Czechowski, 2012). The temperature uniformly exceeds 260 K up to 0.8×satellite's radius from the center, and the molten region extends to 0.5×satellite's radius. The temperature difference between the center and the surface induces an intensive convection of water-rock mixture which flattens the temperature distribution. The radius of the molten region critically depends on the amount of ^{26}Al present at the beginning. The decay of ^{26}Al leads to the melting of Enceladus with a radius of 250 km (Schubert *et al*., 2007) and the small satellite Phoebe, 106 km in radius (Castillo-Rogez *et al*., 2012). Even if ^{26}Al is depleted upon the formation of an icy object, the decay of a long-lived radionuclide can induce the melting, provided that the ice contains $\sim$ 10 weight % ammonia (Nagel *et al*., 2004; Multhaup and Spohn, 2007).

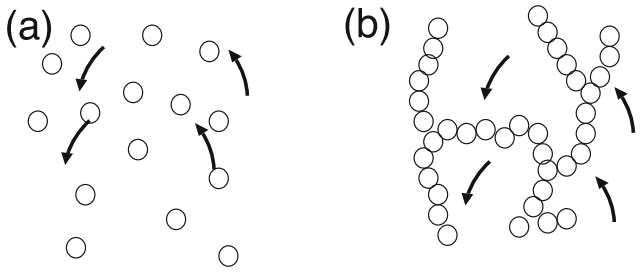

Fig. 2. Schematics of convection in a water-silicate particle mixture. (a) Convection in the absence of coagulation. Both water and silicate particles freely convect. (b) Coagulation in the presence of coagulation. A network of silicate particles is formed. Water convects permeably inside the network.

Let us assume a molten layer of thickness D composed of water and silicate particles which is formed by a heating event. For simplicity, I focus on the stage in which the temperature of the layer is less than the boiling temperature of water. A temperature distribution in the layer promotes a thermal convection flow of water. The Stokes drag force F_d of a flow to a particle of size r is:

$$F_\mathrm{d} = 6\pi\eta r V, \tag{1}$$

where η is the viscosity of water, and V is the relative velocity between the particle and the flow. The balance between F_d and the gravitational force $4\pi\Delta\rho r^3 g/3$, where g is the gravitational acceleration, gives the settling velocity of the particle V_f as:

$$V_\mathrm{f} = \frac{2\Delta\rho g r^2}{9\eta}. \tag{2}$$

If V_f is larger than the upward velocity of the flow, the particle settles down and differentiation proceeds.

First, the case is discussed in which the particles cannot coagulate, due to the repulsive forces between them. In this case, the water and the silicate particles freely flow by means of convection (Fig. 2(a)). Here, a classical expression of the convection velocity V_c in a high Rayleigh-number regime given by (Ahlers *et al*., 2009) is adopted:

$$V_\mathrm{c} \sim \sqrt{\beta\Delta T g D}, \tag{3}$$

where β is the thermal expansion coefficient of water, and ΔT is the temperature variation in the convective layer.

By equating Eqs. (2) and (3), the critical radius r_c above which settling occurs against convective flow is given by:

$$r_\mathrm{c} = \left(\frac{\beta\Delta T D}{g}\right)^{1/4}\left(\frac{9\eta}{2\Delta\rho}\right)^{1/2}. \tag{4}$$

If we assume D is comparable to the size of the icy body, the gravitational acceleration g becomes $4\pi\rho_\mathrm{m} G D/3$, where $\rho_\mathrm{m} = \rho_\mathrm{w}(1-\phi) + \phi\rho_\mathrm{s}$ is the density of the water-silicate mixture. Using these expressions, Eq. (4) can be rewritten as:

$$r_\mathrm{c} = \left(\frac{3\beta\Delta T}{4\pi G\rho_\mathrm{m}}\right)^{1/4}\left(\frac{9\eta}{2\Delta\rho}\right)^{1/2} = 1.2\left(\frac{\Delta T}{10\,\mathrm{K}}\right)^{1/4}\ \mathrm{cm}, \tag{5}$$

where we take $\beta = 2.1\times10^{-4}\,\mathrm{K}^{-1}$, $\rho_\mathrm{s} = 3\,\mathrm{g\,cm}^{-3}$, $\rho_\mathrm{w} = 1.0$ g cm^{-3}, $\Delta\rho = 2.0$ g cm^{-3}, $\phi = 0.33$, and $\eta = 1.0\times10^{-2}$ poise. The temperature dependence of η is neglected. It can be seen that the critical size for settling is substantially larger than the original micron size.

3.2 Setting under coagulation

If coagulation of the particles takes place, the particles connect to each other to form a series of particles (Fig. 1(b)). Further coagulation leads to the formation of a fractal aggregate having a fractal dimension of d. The number of particles of radius r contained in a spherical aggregate of radius r_a is $\sim (r_\mathrm{a}/r)^d$. The aggregate grows through coagulation with other particles or aggregates. Eventually, the aggregates coagulate with each other, such that the total volume of the molten layer V_t is totally spanned with the aggregate. The number of the aggregates in the molten layer V_t is $\sim V_\mathrm{t}/r_\mathrm{a}^3$. If the volume fraction of the particle is ϕ, the total number of particles contained in the molten layer V_t is $\phi V_\mathrm{t}/r^3$ where r is the radius of a particle. From these three relationships, we can obtain $\phi V_\mathrm{t}/r^3 = (r_\mathrm{a}/r)^d(V_\mathrm{t}/r_\mathrm{a}^3)$. From this equation, we have:

$$\phi = (r_\mathrm{a}/r)^{d-3}. \tag{6}$$

The fractal dimension d is $\simeq 2.5$ for a diffusion-limited aggregate (Meakin, 1983). Because the mass ratio between silicate and water is roughly 1:1, based on the solar composition (Greenberg, 1998), the volume fraction of silicate is $\phi \simeq 0.3$, taking into account the density ratio of 3 between silicate and water. In this case, the size of the aggregate becomes $r_\mathrm{a} \simeq 10r$.

The mean collision time of a silicate particle is given by $1/n\sigma v$, where $n = \phi/(4\pi r^3/3)$ is the number density of the silicate particles, $\sigma = \pi(2r)^2$ is the collisional cross-section between two spherical particles of radius r, and $v = \sqrt{kT/(4\pi\rho_\mathrm{s} r^3/3)}$ is the collisional velocity induced by the Brownian motion (ρ_s is the density of a silicate particle). The timescale is $1/n\sigma v = 5.5\times10^{-6}$ s with $r = 0.1\,\mu$m, $T = 300$ K, $\phi = 0.33$, and $\rho_\mathrm{s} = 3.0$ g cm^{-3}. The timescale changes as the aggregates grow. If the aggregates have the same size of r_a, the number density becomes $n/(r_\mathrm{a}/r)^d$, the cross-section is $\sigma(r_\mathrm{a}/r)^2$, and the velocity is $v/(r_\mathrm{a}/r)^{d/2}$, where $(r_\mathrm{a}/r)^d$ is the number of particles contained in an aggregate. The collision timescale for the fractal aggregate of dimension d is then given by $(r_\mathrm{a}/r)^{2-3d/2}/n\sigma v$. The timescale decreases as the aggregate grows, if $d = 2.5$. As a result, the timescale of growth of silicate particles is still roughly given by $1/n\sigma v = 5.5\times10^{-6}$ s. Therefore, the formation of a spanning network is completed shortly after the formation of the molten layer. The typical size of the pore (filled with water) is almost the same as the size of a silicate particle, because the volume fraction of silicate particles is $\phi \simeq 0.3$. When the thermal convection of water takes place, water flows inside these pore spaces.

If the mechanical strength of the network of particles is sufficiently large, the network can sustain its weight against self gravity. Because the network of particles is immersed in water which is in hydrostatic equilibrium, the effective density of the network is $\phi\Delta\rho$, where $\Delta\rho$ is the density difference between silicate and water. Then, the typical pressure applied to the network in a molten layer

inside an object of size R is $\sim G(\phi\Delta\rho)^2R^2 = 2.9 \times 10^8(R/1000\,\mathrm{km})^2\,\mathrm{dyn\,cm^{-2}}$, where G is the gravitational constant, and $\Delta\rho = 2\,\mathrm{g\,cm^{-3}}$ is the density difference between silicate (density $\rho_\mathrm{s} = 3\,\mathrm{g\,cm^{-3}}$) and water (density $\rho_\mathrm{w} = 1\,\mathrm{g\,cm^{-3}}$). The volume fraction of silicate $\phi = 0.33$ is adopted in this formula.

The growth of silicate particles via Ostwald ripening also proceeds in this coagulated case (see Fig. 1(b)). Coagulation of particles forms a neck between them. The neck has a concave surface and low solubility, thereby leading to the precipitation of solutes and to the growth of the neck. As a result, a series of particles loses necks and the local thickness reflects the initial size of the particles (Fig. 1(c)). The strength of the network of grains increases by this growth. Without neck growth, the volume fraction of the aggregates composed of 0.76-μm-radius SiO_2 particles in air increases to $\phi \simeq 0.33$, when a pressure of $\sim 10^7\,\mathrm{dyn\,cm^{-2}}$ is applied (Blum and Schräpler, 2004). Therefore, the strength of the network of grains with growing necks should be larger than this value. A typical compressive strength of oxide ceramics, which is an analogous material to the network of submicron-sized grains with necks grown by sintering, is on the order of $10^9\,\mathrm{dyn\,cm^{-2}}$ (Carter and Norton, 2007). In this case, neither a compaction of the network, nor the differentiation of silicate grains from water, proceeds.

Because the solubility at the relatively thinner section is larger than that at thicker sections (the curvature perpendicular to the network axis is large at a thin section), the thinner part dissolves and shrinks. Eventually, the network is broken at the thinner sections. This fragmentation is a well-known phenomena in the synthesis of monolithic silica from sol-gel reactions (Nakanishi, 2011).

The successive disconnection in the above-mentioned manner produces a fragment that is completely separated from the remaining network of connected particles. A fragment produced by this process settles down provided that the background flow velocity is small. Consequently, the fragment again sticks to the network, and the density, or the packing fraction occupied by the silicate particles, increases.

If the particles coagulate with each other, a network of silicate particles is formed as mentioned in the previous section. In this case, water flows through the network (Fig. 2(b)). The permeable flow velocity V_p is given by Darcy's law (Nield and Bejan, 1998) provided that the Reynolds number is less than one (this is always satisfied), which is written as:

$$V_\mathrm{p} = \frac{K}{\eta}(-\nabla P + \rho_\mathrm{w} g), \tag{7}$$

where K is the permeability of the network, and P is the pressure. The sum on the right-hand side corresponds to the force due to buoyancy, which can be evaluated as $\rho_\mathrm{w} g\beta\Delta T$. The permeability K can be expressed by (Nield and Bejan, 1998):

$$K = \frac{r_\mathrm{f}^2(1-\phi)^3}{180\phi^2}, \tag{8}$$

where r_f is the typical pore size of the network. It should be noted that the thickness r_f grows with time due to ripening, because the size of the unit composing the network increases.

From Eqs. (2) and (7), the critical radius r_p above which settling occurs against permeable flow is given by:

$$r_\mathrm{p} = \frac{9K\beta\Delta T\rho_\mathrm{w}}{2\Delta\rho} = 2.7\times10^{-6}\left(\frac{r_\mathrm{f}}{0.1\,\mu\mathrm{m}}\right)\left(\frac{\Delta T}{10\,\mathrm{K}}\right)^{1/2}\mathrm{cm}, \tag{9}$$

where $\phi = 0.33$ is adopted in the permeability K. It should be noted again that the network radius r_f grows with time. At the beginning, the thickness of the network is on the order of the size of a silicate particle $\sim 0.1\,\mu$m. The thickness of the network increases by ripening. Nevertheless, we can conclude that a fragment can always settle down under any conditions. The minimum size of a fragment is on the order of the network radius r_f. If we set $r_\mathrm{p} = r_\mathrm{f}$ in the left-hand side of Eq. (9), the value of the left-hand side is always larger than that of the right-hand side. The size of the fragment should be larger than r_f, because it is composed of a connected section of the network. Therefore, the settling of particles (fragments from the network in this case) proceeds once the fragmentation of the silicate particle network occurs. By comparing Eqs. (5) and (9), it can be observed that the conditions for settling are easily satisfied in the presence of coagulation, because the flow velocity is small.

4. Timescale for Settling

In the settling process, the molecules constituting a silicate particle dissolve into, and precipitate from, water. As described before, the difference in solubility depending on the surface curvature promotes dissolution from a small particle and precipitation on a large particle. Eventually, the small particle disappears and a relatively thin section in a network of particles disconnects, while a large particle, or a thick section in a network, grows. As a result, the size distribution (or the thickness distribution of a network) of particles evolves.

Because the diffusion timescale of a molecule across the pore space is much shorter than the dissolution (or precipitation) timescale, the concentration of the solvent S_E can be approximated to be uniform in water. Consequently, the precipitation rate is proportional to S_E. The dissolution rate is proportional to the surface-curvature dependent solubility. The growth rate of a particle dr/dt can be written as (Iler, 1979):

$$\frac{dr}{dt} = c_\mathrm{p}S_\mathrm{E} - c_\mathrm{d}S(r,T) = c_\mathrm{d}(fS_\mathrm{E} - S(r,T)), \tag{10}$$

where c_d and c_p are constants independent of the concentration, and $f = c_\mathrm{p}/c_\mathrm{d}$. $S(r,T)$ is the solubility on a surface curvature of radius r, given by:

$$S(r,T) = S_0(T)\exp(r_\mathrm{s}/r), \tag{11}$$

where r_s is a material constant. The solubility increases as r decreases. $S_0(T)$ is the temperature-dependent solubility on a flat surface written as:

$$S_0 = S_{00}\exp(-E/kT), \tag{12}$$

where S_{00} is a constant. For SiO_2, a value of $E/k = 1680\,\mathrm{K}$ is obtained (Iler, 1979). If we adopt this value, the solubility (and, correspondingly, the dissolution rate) varies by a factor of 5 between 0°C and 100°C. This variance is small compared with the pH dependence of the dissolution rate, which is addressed in Section 5. The temperature dependence of solubility is not discussed further in this paper.

Experimentally, the solubility S_0 and the dissolution rate dr/dt are separately determined. The dissolution rate is usually measured as a function of time at a constant temperature: 25 °C in many cases. The data on the temperature dependence of dr/dt is sparse in contrast to that for solubility measured at various temperatures. By using the dissolution rate R_0 at the temperature at which the experiment is conducted, we can fix the constant c_d in Eq. (10) by imposing the condition $dr/dt = -R_0 = -c_\mathrm{d} S_0(T_0)$. Upon combining Eqs. (10) and (11), the growth rate can be written as:

$$\frac{dr}{dt}(T) = \frac{R_0(f S_\mathrm{E} - S(r,T))}{S_0(T_0)} \simeq \frac{R_0}{S_0(T_0)}\left[f S_\mathrm{E} - S_0(T)\left(1+\frac{r_\mathrm{s}}{r}\right)\right]. \quad (13)$$

The last approximation is valid because $r_\mathrm{s}/r \ll 1$. The concentration of the solvent S_E is determined through the total balance of the dissolution and deposition. S_E is not determined here, because it is irrelevant to the timescale of particle ripening.

In a previous study (Kuroiwa and Sirono, 2011), the evolution of the size distribution of icy particles is discussed, where the basic mechanism is sublimation and condensation of H_2O ice. Their study is based on the analytical solution obtained by Kumaran (1998). Because Eq. (13) has the same r dependence as that in their study (Kuroiwa and Sirono, 2011), their result gives the timescale of growth τ_g to a size r as:

$$\tau_\mathrm{g} = \frac{r^2 S_0(T)}{R_0 r_\mathrm{s} S_0(T_0)}. \quad (14)$$

The timescale given by Eq. (14) corresponds to the timescale of the fragmentation of a network of radius r. It is noteworthy that the timescale inevitably involves a large variation, because the solubility greatly differs for different chemical species. For example, the dissolution rate R_0 varies from $5.0 \times 10^{-19}\,\mathrm{cm\,s^{-1}}$ for quartz into pure water, to $2.3 \times 10^{-8}\,\mathrm{cm\,s^{-1}}$ for vitreous silica into 1.0 M HF (Iler, 1979). The dissolution rate of kaolinite is on the order of $\sim 10^{-15}\,\mathrm{cm\,s^{-1}}$ (Yang and Steefel, 2008). The dissolution rate of olivine (Fo_{100}) at 25 °C varies from $\sim 10^{-13}\,\mathrm{cm\,s^{-1}}$ to $\sim 10^{-11}\,\mathrm{cm\,s^{-1}}$ depending on the pH, and an empirical formula as a function of pH (Wogelius and Walther, 1991) is given by:

$$R_0 = 3.90 \times 10^{-10-0.54\mathrm{pH}} + 2.26 \times 10^{-13} + 1.00 \times 10^{-15+0.31\mathrm{pH}}\,\mathrm{cm\,s^{-1}}. \quad (15)$$

Let us suppose a temperature of $T_0 \simeq 300\,\mathrm{K}$ (a commonly adopted value in many dissolution experiments) and that the main component of silicate is olivine. The timescale for $r = 0.1\,\mu\mathrm{m}$ at this temperature is shown in Fig. 3, where

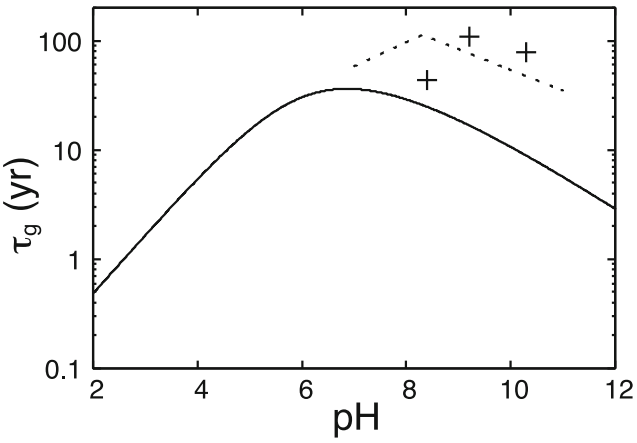

Fig. 3. Timescale for the breakage of a network τ_g for $r = 0.1\,\mu\mathrm{m}$ as a function of pH. The solid line is based on the dissolution rate of olivine at $T = 298\,\mathrm{K}$ (Wogelius and Walther, 1991). The dashed line is for serpentine (Bales and Morgan, 1985). The crosses are the timescale for saponite (Yokoyama and Sato, 2008).

$r_\mathrm{s} = 2 \times 10^{-7}\,\mathrm{cm}$ for vitreous silica (Iler, 1979). This timescale corresponds to the fragmentation of a network radius of $r = 0.1\,\mu\mathrm{m}$. The timescale has a peak at pH $\simeq$ 7 and decreases in both the acidic and basic regions. The timescale is 6.0 yr at the PZC of olivine (pH = 4.1). The timescale is 36 yr at the peak. For comparison, timescales for two major secondary minerals formed by aqueous alterations, serpentine (Bales and Morgan, 1985) and saponite (Yokoyama and Sato, 2008), are shown. The timescales are longer than that for olivine ($\sim$ 100 yr).

These timescales are small compared to the cooling timescale of a molten layer. If the thickness D is larger than $\sqrt{\kappa_\mathrm{ice}\tau_\mathrm{c}} = 55\,\mathrm{m}$, the cooling timescale τ_c is longer than 100 yr and settling is possible. Here, the thermal diffusivity of ice is adopted as $\kappa_\mathrm{ice} = 6.9 \times 10^2/T^2\,\mathrm{cm^2\,s^{-1}}$ with $T = 270\,\mathrm{K}$ (Haruyama *et al.*, 1993).

In the absence of coagulation, the critical size for settling is $\sim$ 1 cm (Eq. (5)). Because $\tau_\mathrm{g} \propto r^2$, the timescale is more than 10^{10} yr. Therefore, if the silicate particles do not coagulate, the probability of differentiation occurring is low.

Two extreme cases, coagulation and without coagulation, have been discussed. Actual internal evolution of an icy body might deviate from these two cases. If the volume fraction of silicate grains ϕ is smaller than the canonical value $\phi = 0.33$, the permeability K (Eq. (8)) becomes large because the low packing fraction enables a high-velocity permeable flow. This effect lowers the critical radius of grains (Eq. (9)). The critical size is larger than the typical grain size 10^{-5} cm if $\phi < 0.22$. Therefore, differentiation is only possible with a high volume fraction of silicate grains.

Another possibility is the fragmentation of the silicate network due to stress generated by the convective flow. A fragment larger than the critical size (Eq. (5)) settles down against the convective flow. However, the porosity inside the fragment does not change by the settlement. To reduce the internal porosity, fragmentation by ripening followed by settling of silicate particles is required.

5. Discussion

As shown in the previous sections, one critical quantity that determines the settling is the pH of the water. Two factors depend on this pH. First, the coagulation of silicate particles is affected by the pH value. The surface of a particle is charged positively or negatively depending on the pH. There is a particular pH called "point of zero charge" (PZC) at which the surface of a particle is neutral. The surface charge increases as the pH deviates from this value. The PZCs for representative silicates are as follows: amorphous silica/quartz 1.8–3.5, feldspar 2.0–2.4, olivine 4.1, kaolinite 3.3–6.0, and serpentine 9.6–11.8 (Parks, 1967). Coagulation proceeds efficiently around the PZC. An electrostatic repulsive force prevents coagulation as the deviation from the PZC increases. This is critical because the probability of differentiation reduces if coagulation does not take place.

The second mechanism involving pH is the dependence of the dissolution rate as seen in Fig. 3. This effect influences the timescale for breaking the network by two orders of magnitude.

The pH of water is determined by water–rock reaction. A calculation of an oceanic composition of Enceladus (Zolotov, 2007) starting from a mixture of water and CI chondrite composition rock showed that the pH of the ocean is alkaline, ranging from 8 to 11. This range of pH would be buffered by secondary minerals (saponite, serpentine) and an abundance of cations formed by aqueous/hydrothermal alterations. The range of pH includes the PZC of serpentine. If this is the case, coagulation of serpentine grains proceeds and differentiation of serpentine from water occurs as a result of ripening. The combination of the secondary minerals and the pH determined from water–rock reaction is critical in the differentiation of an icy body.

6. Conclusion

The differentiation of ice–silicate in icy objects is accompanied by the melting of the object. In order for differentiation to proceed, the size of a silicate particle should be larger than a critical size for which the settling velocity is larger than the background convective velocity of water. In this study, the critical sizes for settling and the timescale for growth of silicate particles to these sizes have been derived. If the silicate particles coagulate with each other in the water-silicate mixture, differentiation is possible because the flow velocity of water is slow. On the other hand, if the silicate particles cannot coagulate because of repulsive forces between them, differentiation does not proceed because the time duration for growth to the critical size for settling is large.

Acknowledgments. The author greatly thanks the constructive comments by two anonymous reviewers. The author is grateful to Dr. Maria Teresa Capria who provided a comfortable stay in Instituto di Astrofisica Spaziale e Fisica Cosmica (Roma), where this work was carried out.

References

Ahlers, G., S. Grossmann, and D. Lohse, Heat transfer and large scale dynamics in turbulent Rayleigh–Benard convection, *Rev. Mod. Phys.*, **81**, 503–537, 2009.

Bales, R. C. and J. J. Morgan, Dissolution kinetics of chrysotile at pH 7 to 10, *Geochim. Cosmochim. Acta*, **49**, 2281–2288, 1985.

Barr, A. C. and R. M. Canup, Origin of Ganymede–Callisto dichotomy by impacts during the late heavy bombardment, *Nat. Geosci.*, **3**, 164–167, 2010.

Blum, J. and R. Schräpler, Structure and mechanical properties of high-porosity macroscopic agglomerates formed by random ballistic deposition, *Phys. Rev. Lett.*, **93**, 115503, 2004.

Carter, C. B. and M. G. Norton, *Ceramic Materials: Science and Engineering*, 738 pp, Springer Science+Business Media, New York, 2007.

Castillo-Rogez, J. C., T. V. Johnson, P. C. Thomas, M. Choukroun, D. L. Matson, and J. I. Lunine, Geophysical evolution of Saturn's satellite Phoebe, a large planetesimal in the outer Solar System, *Icarus*, **219**, 86–109, 2012.

Czechowski, L., Thermal history and large scale differentiation of the Saturn's Satellite Rhea, *Acta Geophys.*, **60**, 1192–1212, 2012.

Eberl, D. D., J. Srodon, M. Kralik, B. E. Taylor, and Z. E. Peterman, Ostwald ripening of clays and metamorphic minerals, *Science*, **248**, 474–477, 1990.

Greenberg, J. M., Making a comet nucleus, *Astron. Astrophys.*, **330**, 375–380, 1998.

Haruyama, J., T. Yamamoto, H. Mizutani, and J. M. Greenberg, Thermal history of comets during residence in the Oort cloud–effect of radiogenic heating in combination with the very low thermal conductivity of amorphous ice, *J. Geophys. Res.,* **98**(E8), 15079, 1993.

Iler, R. K., *The Chemistry of Silica*, 896 pp, John Wiley & Sons, New York, 1979.

Kumaran, V., Effect of convective transport on droplet spinodal decomposition in fluids, *J. Chem. Phys.*, **109**, 2437–2441, 1998.

Kuroiwa, T. and S. Sirono, Evolution of size distribution of icy grains by sublimation and condensation, *Astrophys. J.*, **739**, 18, 2011.

Kuskov, O. L. and V. A. Kronrod, Internal structure of Europa and Callisto, *Icarus*, **177**, 550–569, 2005.

Li, A. and J. M. Greenberg, A unified model of interstellar dust, *Astron. Astrophys.*, **323**, 566–584, 1997.

Meakin, P., Diffusion–controlled cluster formation in 2-6–dimensional space, *Phys. Rev. A*, **27**, 1495–1507, 1983.

Multhaup, K. and T. Spohn, Stagnant lid convection in the mid-sized icy satellites of Saturn, *Icarus*, **186**, 420–435, 2007.

Nagel, K., D. Breuer, and T. Spohn, A model for the interior structure, evolution, and differentiation of Callisto, *Icarus*, **169**, 402–412, 2004.

Nakanishi, K., Synthesis concepts and preparation of silica monoliths, in *Monolithic Silicas in Separation Science*, edited by K. K. Unger, N. Tanaka, and E. Machtejevas, 362 pp, Wiley-VCH Verlag GmBH & Co. KGaA, Weinheim, 2011.

Nield, D. A. and A. Bejan, *Convection in Porous Media*, Springer-Verlag, New York, 1998.

Parks, G. A., Aqueous surface chemistry of oxides and complex oxide minerals, in *Equilibrium Concepts in Natural Water Systems*, edited by W. Stumm, 344 pp, Am. Chem. Soc., Washington, 1967.

Prialnik, D. and R. Merk, Growth and evolution of small porous icy bodies with an adaptive-grid thermal evolution code. I. Application to Kuiper belt objects and Enceladus, *Icarus*, **197**, 211–220, 2008.

Ratke, L. and P. W. Voorhees, *Growth and Coarsening: Ripening in Material Processing*, 295 pp, Springer-Verlag, New York, 2002.

Ross, M. N. and G. Schubert, Tidal heating in an internal ocean model of Europa, *Nature*, **325**, 133–134, 1987.

Safran, A., *Statistical Thermodynamics of Surfaces, Interfaces, and Membranes*, 288 pp, Persens book, Massachusetts, 1994.

Schubert, G., J. D. Anderson, B. J. Travis, and J. Palguta, Enceladus: Present internal structure and differentiation by early and long-term radiogenic heating, *Icarus*, **188**, 345–355, 2007.

Showman, A. P. and R. Malhotra, The Galilean satellites, *Science*, **286**, 77–84, 1999.

Wogelius, R. A. and J. V. Walther, Olivine dissolution at 25 °C: effects of pH, CO_2, and organic acids, *Geochim. Cosmochim. Acta*, **55**, 943–954, 1991.

Yang, L. and C. I. Steefel, Kaolinite dissolution and precipitation kinetics at 22 °C and pH 4, *Geochim. Cosmochim. Acta*, **72**, 99–116, 2008.

Yokoyama, S. and T. Sato, Kinetics study on saponite dissolution under alkaline conditions—Applicability of saponite as engineered barrier for radioactive waste disposal facility—, *Civil Engineering Research Laboratory Report*, No N07020, 2008.

Zolotov, M. Y., An oceanic composition on early and today's Enceladus, *Geophys. Res. Lett.*, **34**, L23203, 2007.

S. Sirono (e-mail: sirono@eps.nagoya-u.ac.jp)